HHS Public Access

Author manuscript

Arterioscler Thromb Vasc Biol. Author manuscript; available in PMC 2016 October 01.

Published in final edited form as:

Arterioscler Thromb Vasc Biol. 2015 October ; 35(10): 2114–2121. doi:10.1161/ATVBAHA.115.306055.

Multi-site thrombus imaging and fibrin content estimation with a single whole-body PET scan in rats

Francesco Blasi, **Bruno L Oliveira**[1], **Tyson A. Rietz**[1], **Nicholas J Rotile**[1], **Pratap C Naha**[2], **David P Cormode**[2], **David Izquierdo-Garcia**[1], **Ciprian Catana**[1], and **Peter Caravan**[1,3]

[1]Athinoula A. Martinos Center for Biomedical Imaging, Massachusetts General Hospital, Harvard Medical School, Charlestown, MA, USA

[2]Department of Radiology, Perelman School of Medicine, University of Pennsylvania, Philadelphia, PA, USA

[3]Institute for Innovation in Imaging, Massachusetts General Hospital, Boston, MA, USA

Abstract

Objective—Thrombosis is a leading cause of morbidity and mortality worldwide. Current diagnostic strategies rely on imaging modalities that are specific for distinct vascular territories, but a thrombus-specific whole-body imaging approach is still missing. Moreover, imaging techniques to assess thrombus composition are underdeveloped, although therapeutic strategies may benefit from such technology. Therefore, our goal was to test whether positron emission tomography (PET) with the fibrin-binding probe ^{64}Cu-FBP8 allows multi-site thrombus detection and fibrin content estimation.

Approach and Results—Thrombosis was induced in Sprague-Dawley rats (n=32) by ferric chloride application on both carotid artery and femoral vein. ^{64}Cu-FBP8-PET/CT imaging was performed 1, 3 or 7 days after thrombosis to detect thrombus location and to evaluate age-dependent changes in target uptake. Ex vivo biodistribution, autoradiography and histopathology were performed to validate imaging results. Arterial and venous thrombi were localized on fused PET/CT images with high accuracy (97.6%, 95% confidence interval: 92–100%). A single whole-body PET/MR imaging session was sufficient to reveal the location of both arterial and venous thrombi after ^{64}Cu-FBP8 administration. PET imaging showed that probe uptake was greater in younger clots than in older ones for both arterial and venous thrombosis ($P<0.0001$). Quantitative histopathology revealed an age-dependent reduction of thrombus fibrin content ($P<0.001$), consistent with PET results. Biodistribution and autoradiography further confirmed the imaging findings.

Conclusions—We demonstrated that ^{64}Cu-FBP8-PET is a feasible approach for whole-body thrombus detection, and that molecular imaging of fibrin can provide, noninvasively, insight into clot composition.

Correspondence: Peter Caravan, PhD, Building 149, Room 2301, 13th Street, Charlestown, MA 02129, USA. Phone 617-643-0193, FAX 617-726-7422, caravan@nmr.mgh.harvard.edu.

Disclosures: Dr. Caravan has equity in Factor 1A, LLC, the company which holds the patent rights of the fibrin-binding peptide used in this study. The other authors report no conflicts relevant to this article.

Keywords

Thrombosis; Imaging; Fibrin; PET

INTRODUCTION

Thrombosis is often the underlying cause of major cardiovascular diseases including heart attack, stroke, and venous thromboembolism, which are leading causes of morbidity and mortality[1]. Current imaging modalities have good sensitivity and specificity, and have been accepted as gold standards for thrombus detection depending on the anatomical location. Particularly, transesophageal echocardiography (TEE) and contrast-enhanced magnetic resonance imaging (MRI) are used to detect thrombi in the cardiac chambers[2], doppler ultrasound has high sensitivity for deep vein thrombosis (DVT)[3], computed tomography (CT) is the gold standard in the diagnosis of pulmonary embolism (PE)[4] and is used to detect the early signs of stroke [5]. However, thrombus imaging would benefit from a whole-body approach capable of detecting multi-site thrombi instead of several examinations, especially for those cardiovascular events (e.g., thromboembolism) where the identification of both culprit embolus and source thrombus is necessary. Moreover, thrombus detection often relies on anatomical and mechanical vascular abnormalities, or on blood flow deficit, rather than directly imaging the target, which may negatively impact the specificity of detection. Furthermore, none of these modalities is informative about the composition of the thrombus, although therapeutic strategies may benefit from such information[6, 7].

Direct targeting of the thrombus components using molecular imaging offers instead a noninvasive solution with high sensitivity and specificity, as well as potential whole-body applications[8, 9]. Several components of the coagulation cascade have been targeted so far with molecular probes, including some specific and abundant thrombus constituents as activated platelets[10, 11] and fibrin[12, 13]. In particular, fibrin is an ideal target for molecular imaging of thrombosis because it is present at high concentrations in both venous and arterial clots but not in circulating blood, resulting in potential high sensitivity and specificity of detection[14]. We recently evaluated several positron emission tomography (PET) probes for noninvasive thrombus detection[15–19] based on fibrin-targeting peptides with high specificity for fibrin over fibrinogen and other plasma proteins[20, 21]. The fibrin-binding probe ^{64}Cu-FBP8 emerged as the best candidate for further translation owing to its high target affinity, fast blood clearance, and high metabolic stability.

Here, we aim to assess the feasibility of ^{64}Cu-FBP8-PET imaging for whole-body thrombus detection in both the venous and arterial circulation at different stages of thrombus evolution following a single administration of probe. Moreover, we also tested whether ^{64}Cu-FBP8-PET could inform thrombus composition by noninvasive evaluation of fibrin content.

MATERIALS AND METHODS

Materials and Methods are available in the online-only Data Supplement.

RESULTS

Detection of arterial and venous thrombi with ^{64}Cu-FBP8-PET

Thrombi were generated in the common carotid artery and femoral vein of 32 Sprague-Dawley rats using the ferric chloride model[22], and thrombus location (right vs. left) was kept undisclosed until the end of the study to assess in a blinded fashion the accuracy of ^{64}Cu-FBP8-PET imaging. Contralateral incisions were performed to create a sham surgical wound, hiding the actual location of the clot. At 1, 3 or 7 days after thrombus induction rats were imaged according to the scheme depicted in Figure 1. Sequential PET scans of the hindlimbs and the neck region revealed in every animal the presence of isolated “hot-spots”. The localization of the radioactivity in PET images was suggestive of the common carotid artery and femoral vein, visualized with CT angiography. Fused PET/CT images confirmed that the isolated “hot-spots” were located in the thrombosed vessels. Some radioactivity was detected at the surgical wound and the excretory organs, as previously reported[15–19]. Blinded analysis of the accuracy of ^{64}Cu-FBP8-PET imaging to detect the thrombus location was performed by two independent readers on a total of 21 animals. One reader correctly detected the location of 40 thrombi out of 42 (1d, 14/14; 3d, 14/14; 7d, 12/14), while the other correctly detected the location of all clots (42/42). The mean overall accuracy was 97.6% (82/84), with an exact 95% confidence interval (CI) ranging from 0.916 to 0.997.

To further demonstrate that ^{64}Cu-FBP8-PET is suitable for multi-site thrombus detection with a single whole-body scan, we imaged a small cohort of rats in a clinical PET/MR scanner 1 day after thrombosis, as previously described[15, 16]. Rats were imaged for 60 min starting 1 hour after ^{64}Cu-FBP8 injection (Figure 2). The location of both arterial and venous thrombi was clearly identified in this wide field of view after a single administration of ^{64}Cu-FBP8. Background activity was only detected in the liver, surgical wounds and excretory organs.

^{64}Cu-FBP8 uptake in arterial and venous thrombi depends on thrombus age

^{64}Cu-FBP8-PET imaging revealed that the radioactive signal for both arterial and venous thrombi was dependent on thrombus age. Signal intensity was greatest in 1d old thrombi and gradually declined with thrombus age, with a statistically significant difference among the three groups ($P<0.0001$, 1-way ANOVA, Figure 3). Particularly, we observed 0.65 %ID/cc ± 0.19 SD (1d), 0.35 ± 0.16 (3d), 0.06 ± 0.02 (7d) for the arterial clots, and 0.55 %ID/cc ± 0.15 SD (1d), 0.36 ± 0.05 (3d), 0.12 ± 0.04 (7d) for the venous thrombi. Contralateral carotid artery and femoral vein did not show any radioactive signal that could suggest the presence of a thrombus. Some activity was detected at the surgical wound, excretory organs and genital area, the latter consistent with urine contamination. The high thrombus uptake combined with the low off-target background resulted in high target-to-background ratios. For the arterial thrombus we found 20–30 fold at 1d after surgery, 10–20 fold at 3d, and 2–4 fold differences at 7d, while for the venous clots we observed, 10–20, 5–10 and 2–4 fold at 1, 3 and 7d after thrombosis, respectively. Since the arteries were imaged more than one hour after the veins, and because ^{64}Cu-FBP8 progressively clears from background tissues but shows steady levels at the target site[18], this difference in target-to-background ratios between arterial and venous thrombi is expected based on the timing of the imaging.

Ex vivo biodistribution, autoradiography and histopathology

Animals were euthanized at the end of the imaging experiments, and tissues harvested and processed for biodistribution, autoradiography and histopathology. The presence and the location (left vs. right) of the thrombi in the carotid artery and femoral vein were confirmed in every animal. Biodistribution analysis showed that probe uptake was highest in the younger thrombi for both arterial and venous clots (Figure 4). In particular, the uptake of the arterial thrombi was 1.17 %ID/g ± 0.39 SD at 1d, 0.66 ± 0.36 at 3d and 0.20 ± 0.19 at 7d, while the activity at the level of the venous thrombi was 1.46 ± 0.76 at 1d, 0.96 ± 0.65 at 3d and 0.21 ± 0.10 at 7d. Pearson's analysis showed a positive correlation between the probe uptake detected with gamma-counting and PET quantification, a further validation of the imaging findings. Ex vivo autoradiography showed results comparable to PET imaging and gamma-counting. A hyperintense region was detected in the thrombosed vessels, but not contralaterally. Autoradiography performed on histological slices confirmed the high activity of ipsilateral vessels, corresponding to the H&E-stained thrombus, and very low activity in contralateral arteries and veins. Quantitative assessments revealed high ipsilateral:contralateral activity ratios for arterial and venous thrombi, with a trend comparable to PET imaging and biodistribution. We observed higher ipsi:contra ratios for the younger thrombi (artery 1d, 15 fold; artery 3d, 10 fold; vein 1d, 35 fold; vein 3d, 15 fold) than for the older ones (artery 7d, 3 fold; vein 7d, 5 fold). Histopathology revealed time-dependent changes of thrombus size and composition for both arterial and venous clots ($P<0.001$, 1-way ANOVA, Figure 5). Martius Scarlet Blue (MSB)[24] staining showed that thrombi were conspicuous at 1d and 3d after surgery, while at 7d the clots comprised a lesser extent of the vessel. Fibrin was a major constituent of both arterial and venous thrombi, confirmed by histochemical and immunofluorescence stainings. Younger thrombi (1d and 3d) were rich in fibrin (purple-red) and erythrocytes (yellow), whereas some collagen fibers (blue) were also present at 7d. Color segmentation was performed on MSB-stained sections to quantitatively assess the thrombus composition[25–27] The fibrin content peaked at 1d post-thrombosis for both carotid artery and femoral vein, and gradually decreased over time along with the thrombus size. At 7 days after thrombosis, the fibrin content in venous thrombi was greater than in arterial clots, consistent with the difference in uptake observed with PET imaging. In particular, the fibrin content was 0.74 mm^3 ± 0.25 SD at 1d, 0.39 ± 0.18 at 3d and 0.08 ± 0.03 at 7d for arterial thrombi, and 0.83 mm^3 ± 0.26 SD, 0.49 ± 0.09 and 0.19 ± 0.06 at 1d, 3d and 7d for the venous clots, respectively. A positive correlation was found between the probe uptake detected with PET and fibrin content in arterial and venous thrombi ($r=0.75$, $P=0.005$).

DISCUSSION

The aim of this study was to assess the feasibility and potential of ^{64}Cu-FBP8-PET for whole-body thrombus detection and fibrin content estimation. We recently demonstrated that ^{64}Cu-FBP8 has high target uptake, rapid systemic clearance, and low off-target retention in an animal model of hyperacute mural arterial thrombosis[18]. In the present work, we extended our findings to other clinically relevant time-points by imaging the acute and subacute stages of thrombus evolution in both arteries and veins. We first showed that ^{64}Cu-FBP8-PET is suitable for imaging multiple thrombi in different vascular territories and

anatomical locations (neck and hindlimbs), with an overall accuracy >97%. The high probe uptake, combined with the fast off-target washout, allowed detection of arterial and venous thrombi with high target-to-background ratios. Then, we assessed whether ^{64}Cu-FBP8-PET can provide insights on thrombus age and composition by evaluation of fibrin content. Our findings showed that probe uptake was higher for the younger clots and lower for the older ones, and that such age-dependent uptake was consistent with the amount of fibrin in these thrombi. Taken together, these results provide a proof-of-concept for a new, sensitive approach based on PET imaging for whole-body thrombus detection and to noninvasively assess changes in thrombus composition by directly targeting its main component: fibrin.

Despite the recent advances in noninvasive thrombus detection, current imaging modalities still have some limitations that challenge both diagnosis and therapy monitoring. A main diagnostic drawback is the absence of a single-session approach with high sensitivity and specificity to detect thrombosis in different anatomical locations. In fact, sensitivity and specificity of current imaging modalities depend on the anatomical location of the thrombus[2–5]. However in the case of thromboembolism both diagnosis and therapeutic strategy would benefit from a single approach with whole-body detection capabilities to reveal the location of the culprit embolus (e.g., middle cerebral artery in case of stroke, pulmonary artery in case of PE) as well as the source thrombus (e.g., atherosclerotic carotid plaque, aortic arch, left atrial thrombus, DVT). Indeed, a potential application for ^{64}Cu-FBP8-PET is secondary stroke prevention. The diagnosis of stroke etiology is crucial for secondary prevention since the risk of recurrences is associated with the underlying pathology[28]. Current stroke diagnostic work-up includes ultrasonography, TEE, MR and CT angiography to detect common embolic sources (e.g., aortic arch and intra/extracranial atheroma, atrial thrombi), resulting in a time-consuming and expensive process that can delay therapeutic intervention[29]. Despite these different diagnostic tools, a third of ischemic strokes are classified as cryptogenic (i.e., the source thrombus is unknown)[30]. A whole-body approach would be beneficial in this large population. Earlier work with ^{64}Cu-FBP7, a close analog of ^{64}Cu-FBP8, detected carotid thrombi and intra/extracranial emboli with high target-to-background ratios, and we anticipate similar efficacy with ^{64}Cu-FBP8[17]. Therefore, if translated to a clinical setting, ^{64}Cu-FBP8-PET may help identify the location of both the culprit embolus (e.g., middle cerebral artery) and the source thrombus (e.g., carotid artery, aortic arch) in stroke patients.

Thrombus evolution is a dynamic process, and changes in fibrin content can affect clot stability. Human thrombi are characterized by platelets and fibrin in the early phase, while smooth muscle cells, proteoglycans and collagen are main constituents of healing clots[31, 32]. Fresh clots are usually softer, unstable, and are more likely to be lysed than mature, organized thrombi[33]. Therefore, noninvasive assessment of clot composition can be useful for thrombus staging and to facilitate therapeutic choices (e.g., thrombolysis vs. thrombectomy)[6, 7]. Several attempts have been made to characterize thrombus composition using noninvasive imaging. Ultrasound elastography has shown thrombus staging capabilities ex vivo[34], but its feasibility still needs to be addressed in vivo. Changes in T_1 relaxation time, magnetization transfer and diffusion-weighted MRI have been associated with iron metabolism and protein turnover of venous thrombi, showing diagnostic potential to assess thrombus age and predict successful clot lysis[25, 26]. However, non-contrast MR

imaging offers limited target sensitivity and specificity, and therefore detecting small thrombotic events may be challenging especially for whole-body applications. Molecular MR imaging using the fibrin-binding probe EP-2104R has shown good correlation with fibrin thrombus content[27]. However, molecular MRI requires pre- and post-contrast imaging sessions, which can delay the diagnostic work-flow. Moreover, previous experience with EP-2104R in patients with thrombosis revealed that the clots appears more conspicuous at later time points after injection (24 hours)[35], which may complicate the analysis of pre- and post-probe images and further delay decision-making and treatment. Scintigraphy with the ^{99m}Technetium-labeled activated platelets inhibitor DPM-444[10] and ^{99m}Technetium-rtPA[36] have shown good feasibility identifying fresh clots over organized thrombi, but at the same time the low efficacy in detecting mature clots reduced their clinical applications. Fluorodeoxyglucose (FDG)-PET has been recently used to stage thrombosis by imaging neutrophilic infiltration in fresh venous thrombi[37]. However, FDG uptake is also increased in other pathologies associated with high cellularity and hypermetabolism (e.g., cancer, chronic inflammatory conditions), which may limit the specificity of this imaging approach. The findings shown here demonstrate that ^{64}Cu-FBP8-PET can detect differences in fibrin content in both arterial and venous clots, even when thrombi were small and fibrin levels low (i.e., 7d old thrombi). Because the high target specificity of molecular imaging and the great sensitivity and absolute quantification capabilities of PET, thrombus imaging with ^{64}Cu-FBP8 may overcome the shortcomings of previous imaging modalities and thus provide a novel approach for whole-body clot detection and fibrin content estimation.

This work has some limitations, including the small sample size. We tested our hypothesis in animal models that only partially mimic the human pathology; therefore, our results need to be validated in clinical settings. Moreover, this approach may not be suitable for diagnosis of thrombosis in the emergency department, where minutes of delay negatively impact the clinical outcome. However, ^{64}Cu-FBP8-PET may be beneficial when the life-threatening culprit is under control, but the source thrombus is still unknown and the risk of recurrence is high. In these circumstances, a thrombus imaging approach with whole-body clot detection capabilities may provide useful insight for both diagnosis (e.g., etiological assessment) and intervention. PET imaging has higher costs compared to other modalities and exposes the patient to ionizing radiation. However, the high sensitivity of PET allows using micrograms of tracer compared to other contrast-based imaging modalities where grams of probe are required (e.g., MRI), thus reducing potential chemical toxicity. Despite the relatively long half-life of ^{64}Cu (12.7 h), the rapid whole-body clearance and low retention of ^{64}Cu-FBP8 suggest that radiogenic adverse effects should not limit its clinical translation[18], and recent radiation dosimetry studies in rats support this conclusion[38]. Moreover, the longer half-life may allow synthesis of the molecular probe in advance, and even on demand shipment to remote sites far from a cyclotron. Finally, since its straightforward radiolabeling procedure, ^{64}Cu-FBP8 is also amenable to kit formulation which may further facilitate bench-to-bedside translation.

Conclusions

^{64}Cu-FBP8-PET is a feasible approach for whole-body thrombus detection and for noninvasive evaluation of fibrin content, and represents a novel and valuable diagnostic strategy for translation in clinical imaging of thrombosis.

Supplementary Material

Refer to Web version on PubMed Central for supplementary material.

Acknowledgments

Sources of Funding: this work was supported by HL109448 from the National Heart, Lung, and Blood Institute. The National Center for Research Resources (RR029495) and the Office of the Director (OD010650) at NIH are acknowledged for funding instrumentation used.

References

1. Go AS, Mozaffarian D, Roger VL, et al. Heart disease and stroke statistics--2014 update: a report from the American Heart Association. Circulation. 2014; 129:e28–e292. [PubMed: 24352519]
2. Srichai MB, Junor C, Rodriguez LL, Stillman AE, Grimm RA, Lieber ML, Weaver JA, Smedira NG, White RD. Clinical, imaging, and pathological characteristics of left ventricular thrombus: a comparison of contrast-enhanced magnetic resonance imaging, transthoracic echocardiography, and transesophageal echocardiography with surgical or pathological validation. Am Heart J. 2006; 152:75–84. [PubMed: 16824834]
3. Pomero F, Dentali F, Borretta V, Bonzini M, Melchio R, Douketis JD, Fenoglio LM. Accuracy of emergency physician-performed ultrasonography in the diagnosis of deep-vein thrombosis: a systematic review and meta-analysis. Thromb Haemost. 2013; 109:137–145. [PubMed: 23138420]
4. Fedullo PF, Tapson VF. Clinical practice. The evaluation of suspected pulmonary embolism. N Engl J Med. 2003; 349:1247–1256. [PubMed: 14507950]
5. Moulin T, Cattin F, Crepin-Leblond T, Tatu L, Chavot D, Piotin M, Viel JF, Rumbach L, Bonneville JF. Early CT signs in acute middle cerebral artery infarction: predictive value for subsequent infarct locations and outcome. Neurology. 1996; 47:366–375. [PubMed: 8757006]
6. Silvain J, Collet JP, Nagaswami C, Beygui F, Edmondson KE, Bellemain-Appaix A, Cayla G, Pena A, Brugier D, Barthelemy O, Montalescot G, Weisel JW. Composition of coronary thrombus in acute myocardial infarction. J Am Coll Cardiol. 2011; 57:1359–1367. [PubMed: 21414532]
7. Mehta BP, Nogueira RG. Should clot composition affect choice of endovascular therapy? Neurology. 2012; 79:S63–67. [PubMed: 23008415]
8. Buxton DB, Antman M, Danthi N, et al. Report of the National Heart, Lung, and Blood Institute working group on the translation of cardiovascular molecular imaging. Circulation. 2011; 123:2157–2163. [PubMed: 21576680]
9. Lindner JR. Molecular imaging of thrombus: technology in evolution. Circulation. 2012; 125:3057–3059. [PubMed: 22647974]
10. Mitchel J, Waters D, Lai T, White M, Alberghini T, Salloum A, Knibbs D, Li D, Heller GV. Identification of coronary thrombus with a IIb/IIIa platelet inhibitor radiopharmaceutical, technetium-99m DMP-444: A canine model. Circulation. 2000; 101:1643–1646. [PubMed: 10758044]
11. Wang X, Hagemeyer CE, Hohmann JD, Leitner E, Armstrong PC, Jia F, Olschewski M, Needles A, Peter K, Ahrens I. Novel single-chain antibody-targeted microbubbles for molecular ultrasound imaging of thrombosis: validation of a unique noninvasive method for rapid and sensitive detection of thrombi and monitoring of success or failure of thrombolysis in mice. Circulation. 2012; 125:3117–3126. [PubMed: 22647975]

12. Botnar RM, Perez AS, Witte S, et al. In vivo molecular imaging of acute and subacute thrombosis using a fibrin-binding magnetic resonance imaging contrast agent. Circulation. 2004; 109:2023–2029. [PubMed: 15066940]
13. Morris TA, Gerometta M, Yusen RD, White RH, Douketis JD, Kaatz S, Smart RC, Macfarlane D, Ginsberg JS. Detection of pulmonary emboli with 99mTc-labeled anti-D-dimer (DI-80B3)Fab′ fragments (ThromboView). Am J Respir Crit Care Med. 2011; 184:708–714. [PubMed: 21680946]
14. Ciesienski KL, Caravan P. Molecular MRI of Thrombosis. Curr Cardiovasc Imaging Rep. 2010; 4:77–84. [PubMed: 21253438]
15. Uppal R, Catana C, Ay I, Benner T, Sorensen AG, Caravan P. Bimodal thrombus imaging: simultaneous PET/MR imaging with a fibrin-targeted dual PET/MR probe--feasibility study in rat model. Radiology. 2011; 258:812–820. [PubMed: 21177389]
16. Ciesienski KL, Yang Y, Ay I, Chonde DB, Loving GS, Rietz TA, Catana C, Caravan P. Fibrin-targeted PET probes for the detection of thrombi. Mol Pharm. 2013; 10:1100–1110. [PubMed: 23327109]
17. Ay I, Blasi F, Rietz TA, Rotile NJ, Kura S, Brownell AL, Day H, Oliveira BL, Looby RJ, Caravan P. In vivo molecular imaging of thrombosis and thrombolysis using a fibrin-binding positron emission tomographic probe. Circ Cardiovasc Imaging. 2014; 7:697–705. [PubMed: 24777937]
18. Blasi F, Oliveira BL, Rietz TA, Rotile NJ, Day H, Looby RJ, Ay I, Caravan P. Effect of Chelate Type and Radioisotope on the Imaging Efficacy of 4 Fibrin-Specific PET Probes. J Nucl Med. 2014; 55:1157–1163. [PubMed: 24790217]
19. Boros E, Rybak-Akimova E, Holland JP, Rietz T, Rotile N, Blasi F, Day H, Latifi R, Caravan P. Pycup--a bifunctional, cage-like ligand for (64)Cu radiolabeling. Mol Pharm. 2014; 11:617–629. [PubMed: 24294970]
20. Kolodziej AF, Nair SA, Graham P, McMurry TJ, Ladner RC, Wescott C, Sexton DJ, Caravan P. Fibrin specific peptides derived by phage display: characterization of peptides and conjugates for imaging. Bioconjug Chem. 2012; 23:548–556. [PubMed: 22263840]
21. Overoye-Chan K, Koerner S, Looby RJ, Kolodziej AF, Zech SG, Deng Q, Chasse JM, McMurry TJ, Caravan P. EP-2104R: a fibrin-specific gadolinium-Based MRI contrast agent for detection of thrombus. J Am Chem Soc. 2008; 130:6025–6039. [PubMed: 18393503]
22. Kurz KD, Main BW, Sandusky GE. Rat model of arterial thrombosis induced by ferric chloride. Thromb Res. 1990; 60:269–280. [PubMed: 2087688]
23. Loening AM, Gambhir SS. AMIDE: a free software tool for multimodality medical image analysis. Mol Imaging. 2003; 2:131–137. [PubMed: 14649056]
24. Lendrum AC, Fraser DS, Slidders W, Henderson R. Studies on the character and staining of fibrin. J Clin Pathol. 1962; 15:401–413. [PubMed: 13929601]
25. Saha P, Andia ME, Modarai B, et al. Magnetic resonance T1 relaxation time of venous thrombus is determined by iron processing and predicts susceptibility to lysis. Circulation. 2013; 128:729–736. [PubMed: 23820077]
26. Phinikaridou A, Andia ME, Saha P, Modarai B, Smith A, Botnar RM. In vivo magnetization transfer and diffusion-weighted magnetic resonance imaging detects thrombus composition in a mouse model of deep vein thrombosis. Circ Cardiovasc Imaging. 2013; 6:433–440. [PubMed: 23564561]
27. Andia ME, Saha P, Jenkins J, Modarai B, Wiethoff AJ, Phinikaridou A, Grover SP, Patel AS, Schaeffter T, Smith A, Botnar RM. Fibrin-targeted magnetic resonance imaging allows in vivo quantification of thrombus fibrin content and identifies thrombi amenable for thrombolysis. Arterioscler Thromb Vasc Biol. 2014; 34:1193–1198. [PubMed: 24723557]
28. Purroy F, Montaner J, Molina CA, Delgado P, Ribo M, Alvarez-Sabin J. Patterns and predictors of early risk of recurrence after transient ischemic attack with respect to etiologic subtypes. Stroke. 2007; 38:3225–3229. [PubMed: 17962602]
29. Schaer B, Sticherling C, Lyrer P, Osswald S. Cardiological diagnostic work-up in stroke patients--a comprehensive study of test results and therapeutic implications. Eur J Neurol. 2009; 16:268–273. [PubMed: 19146645]

30. Guercini F, Acciarresi M, Agnelli G, Paciaroni M. Cryptogenic stroke: time to determine aetiology. J Thromb Haemost. 2008; 6:549–554. [PubMed: 18208534]

31. Fuster V, Fayad ZA, Moreno PR, Poon M, Corti R, Badimon JJ. Atherothrombosis and high-risk plaque: Part II: approaches by noninvasive computed tomographic/magnetic resonance imaging. J Am Coll Cardiol. 2005; 46:1209–1218. [PubMed: 16198833]

32. Kramer MC, Rittersma SZ, de Winter RJ, Ladich ER, Fowler DR, Liang YH, Kutys R, Carter-Monroe N, Kolodgie FD, van der Wal AC, Virmani R. Relationship of thrombus healing to underlying plaque morphology in sudden coronary death. J Am Coll Cardiol. 2010; 55:122–132. [PubMed: 19818571]

33. Brommer EJ, Potter van Loon BJ, Rijken DC, van Bockel JH. Composition and susceptibility to thrombolysis of pathological human arterial thrombi. Ann N Y Acad Sci. 1992; 667:283–285. [PubMed: 1309047]

34. Geier B, Barbera L, Muth-Werthmann D, Siebers S, Ermert H, Philippou S, Mumme A. Ultrasound elastography for the age determination of venous thrombi. Evaluation in an animal model of venous thrombosis. Thromb Haemost. 2005; 93:368–374. [PubMed: 15711756]

35. Vymazal J, Spuentrup E, Cardenas-Molina G, Wiethoff AJ, Hartmann MG, Caravan P, Parsons EC Jr. Thrombus imaging with fibrin-specific gadolinium-based MR contrast agent EP-2104R: results of a phase II clinical study of feasibility. Invest Radiol. 2009; 44:697–704. [PubMed: 19809344]

36. Brighton T, Janssen J, Butler SP. Aging of acute deep vein thrombosis measured by radiolabeled 99mTc-rt-PA. J Nucl Med. 2007; 48:873–878. [PubMed: 17504873]

37. Hara T, Truelove J, Tawakol A, Wojtkiewicz GR, Hucker WJ, MacNabb MH, Brownell AL, Jokivarsi K, Kessinger CW, Jaff MR, Henke PK, Weissleder R, Jaffer FA. 18F-fluorodeoxyglucose positron emission tomography/computed tomography enables the detection of recurrent same-site deep vein thrombosis by illuminating recently formed, neutrophil-rich thrombus. Circulation. 2014; 130:1044–1052. [PubMed: 25070665]

38. Blasi F, Oliveira BL, Rietz TA, Rotile NJ, Day H, Naha PC, Cormode DP, Izquierdo-Garcia D, Catana C, Caravan P. Radiation Dosimetry of the Fibrin-Binding Probe 64Cu-FBP8 and Its Feasibility for PET Imaging of Deep Vein Thrombosis and Pulmonary Embolism in Rats. J Nucl Med. 2015; 56:1088–1093. [PubMed: 25977464]

SIGNIFICANCE

Thrombosis is the underlying cause of deadly diseases such as stroke, pulmonary embolism, deep vein thrombosis, and heart attack, which affect millions of people worldwide. Current thrombus imaging techniques are specific for selected anatomical locations, but whole-body detection of thrombi with a single scan is not feasible yet. Therefore, the diagnosis of cardiovascular diseases where multiple thrombi are hidden, and ready to generate deadly emboli, requires several diagnostic assessments, which may delay both diagnosis and therapeutic intervention. Molecular imaging of thrombosis using positron emission tomography (PET) and the fibrin-specific probe FBP8 allows sensitive and specific whole-body detection of thrombi with a single scan providing a novel and powerful tool that may facilitate diagnosis, guide therapeutic choices, and monitor treatment efficacy.

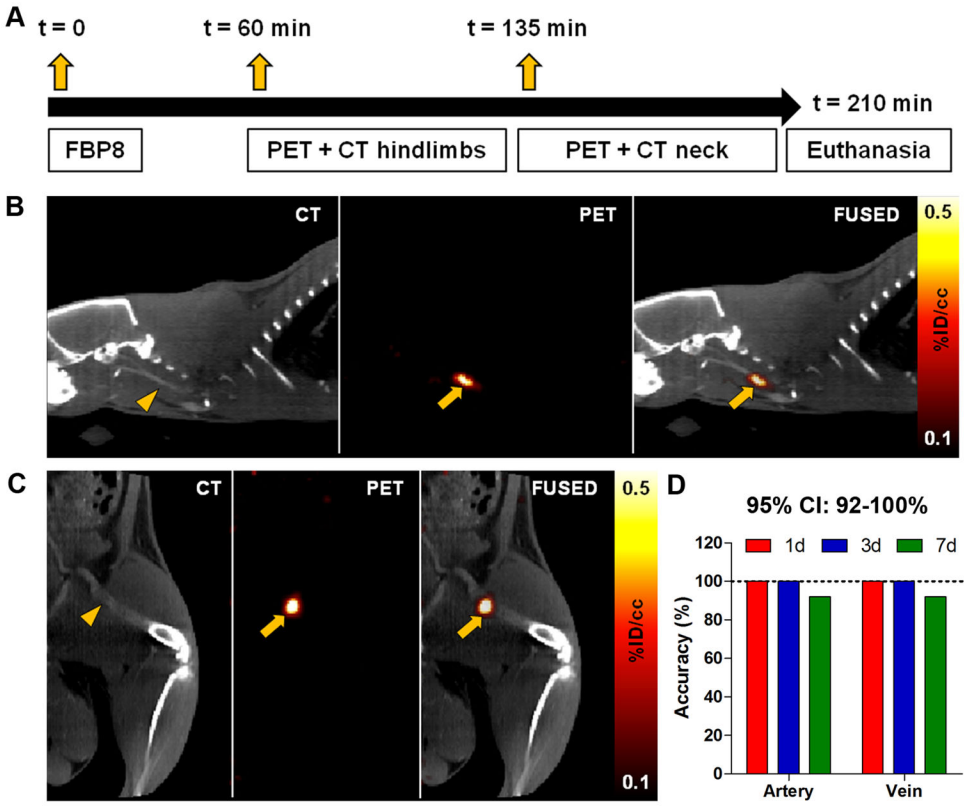

Figure 1. Molecular imaging of arterial and venous thrombosis with ^{64}Cu-FBP8-PET/CT

Experimental scheme showing probe administration and imaging time-points (A). CT, PET, and fused images from a representative animal injected with a single dose of ^{64}Cu-FBP8 three days after the induction of arterial (B) and venous (C) thrombosis. Contrast-enhanced CT angiography was used to detect the common carotid artery (B, arrowhead) and the femoral vein (C, arrowhead). The thrombus location appears as a hot-spot on the ipsilateral carotid artery (B, arrows) and femoral vein (C, arrows). Blinded assessment of PET accuracy to detect the location of the clot (right vs. left) performed by two independent investigators (D). n=7/group.

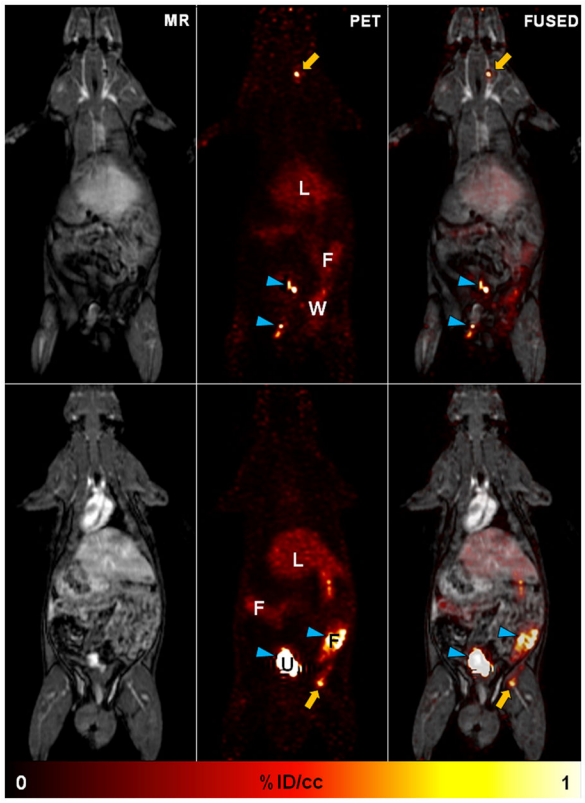

Figure 2. Whole-body thrombus detection with ^{64}Cu-FBP8-PET/MR

Whole-body images from a representative rat injected with ^{64}Cu-FBP8 one day after thrombosis. Simultaneous PET/MR imaging was performed in a clinical scanner starting 1 hour after probe administration. Thrombus location (arrows) was detected in the right carotid artery (top) and right femoral vein (bottom). Radioactivity in urine and feces (arrowheads) is off-scale. L, liver; F, fecal matter; U, urine; W, surgical wound. n=2.

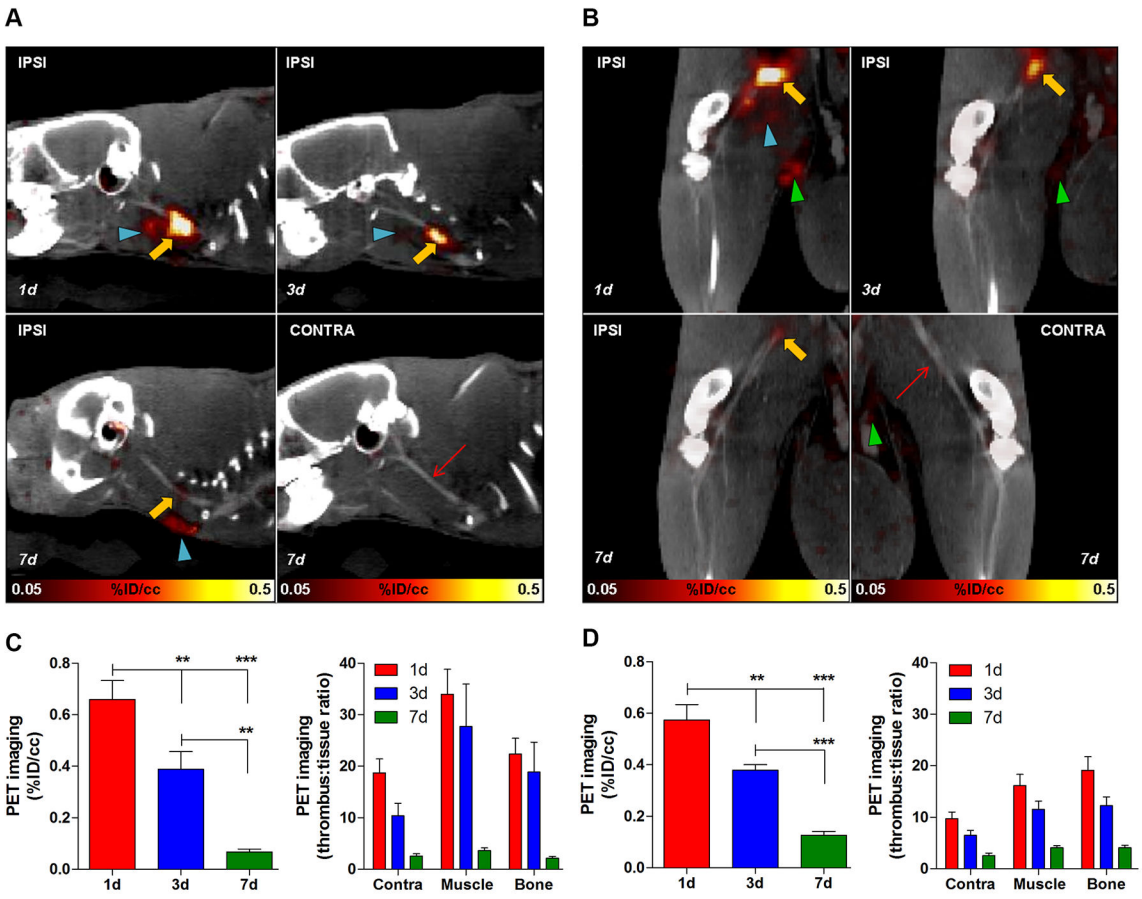

Figure 3. ^{64}Cu-FBP8-PET reveals age-dependent changes in thrombus uptake

Fused PET/CT images of representative rats injected with ^{64}Cu-FBP8 showing age-dependent decrease in arterial (A) and venous (B) thrombus uptake. No uptake was detected in the contralateral vessels (contra). PET quantification reveals statistically significant differences in thrombus uptake among groups and high target-to-background tissues ratios for both arterial (C) and venous (D) thrombi. Ipsi, ipsilateral; contra, contralateral. Thrombus, yellow arrow; contralateral vessel, red thin arrow; surgical wound, blue arrowheads; urine, green arrowheads. Error bars are SEM. ***P<0.001 and **P<0.01, 1-way ANOVA followed by Tukey post-hoc test. n=7/group.

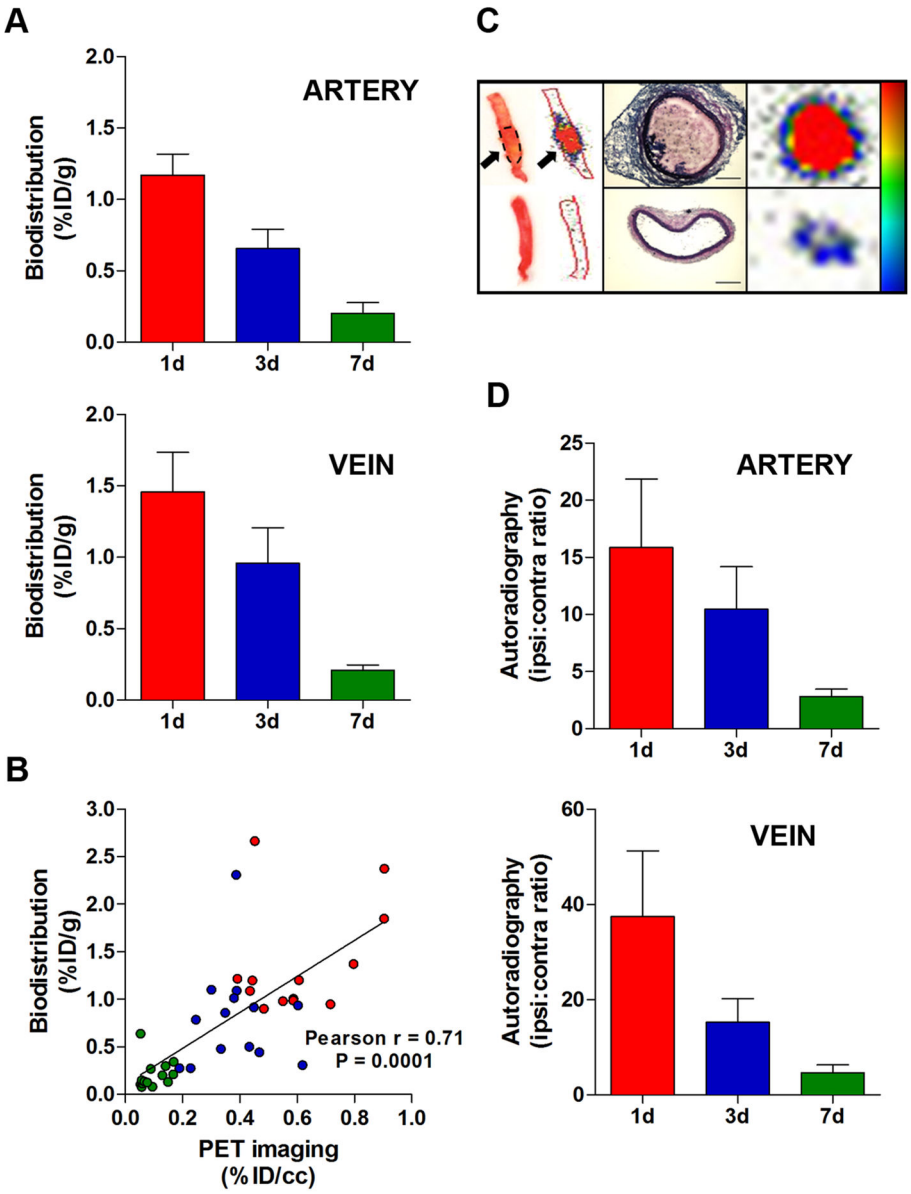

Figure 4. Biodistribution and autoradiography

Gamma-counting of thrombosed arteries and veins showed age-dependent reduction of thrombus uptake (A). Positive correlation between thrombus uptake assessed with PET imaging and gamma-counting (B). Representative images and relative autoradiograms of thrombosed carotid arteries showing high uptake at the thrombus site (arrows) but only low activity in the contralateral vessel (C, left panel). The high activity of the thrombosed vessel (C, right panel) corresponds to the intraluminal thrombus and not the vascular tunica, as shown by H&E-stained histological sections (C, middle panel). Ipsilateral-to-contralateral activity ratios of thrombosed arteries and veins revealed high target-to-background contrast which gradually decreased over time, consistent with reduction of target uptake (D). Scale bars: 0.2 mm. Error bars are SEM. Biodistribution, n=7/group. Autoradiography, n=5/group.

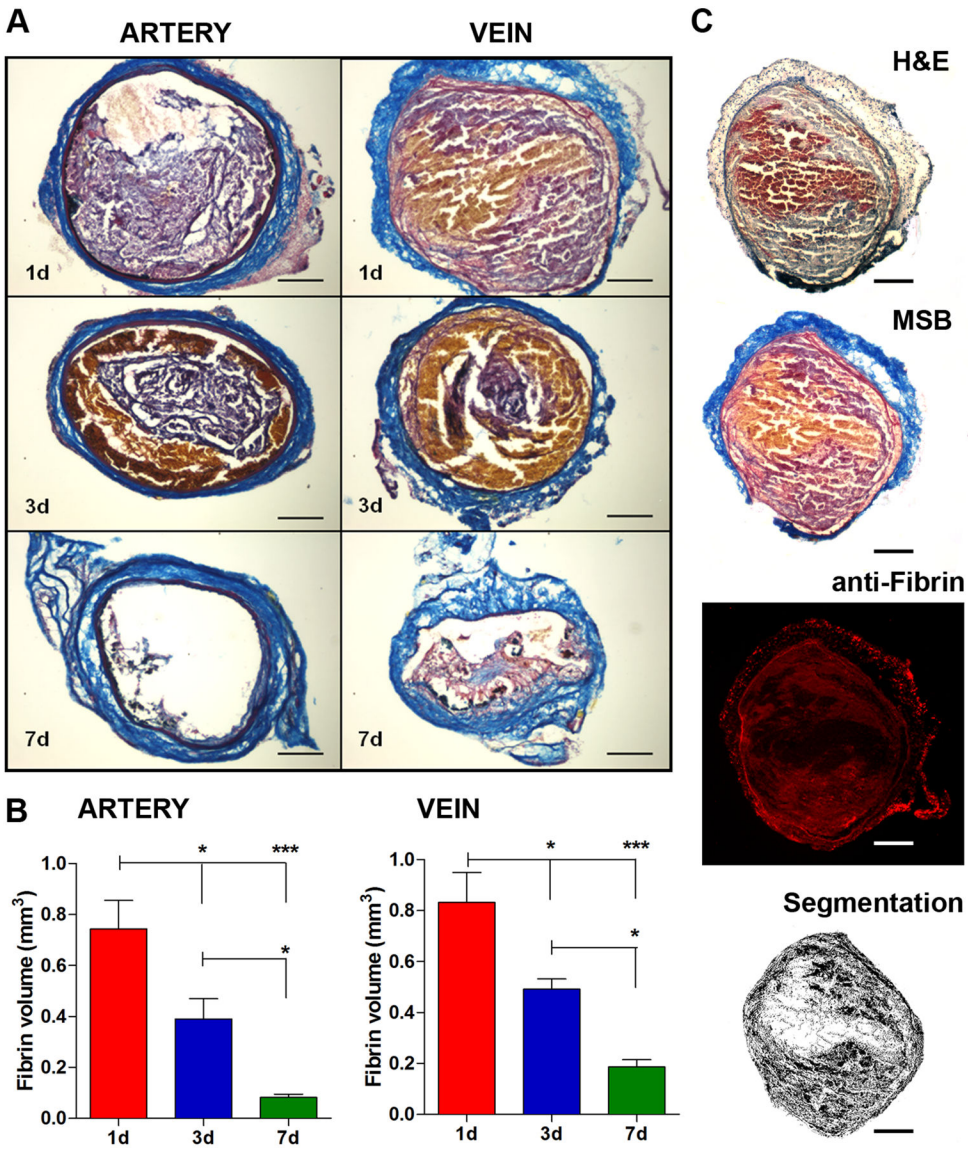

Figure 5. Histopathology

Representative coronal sections of arterial and venous thrombi stained with MSB showing time-dependent changes in thrombus size and composition (A). Volumetric quantification of thrombus composition revealed a gradual reduction of fibrin content (B). Adjacent histological sections stained with Hematoxylin&Eosin, Martius Scarlet Blue and anti-fibrin antibody showed congruent localization of fibrin, confirming the selectivity of MSB staining for fibrin (C). Color segmentation analysis performed on the MSB-stained section shows fibrin detection. Scale bars: 0.2 mm. Error bars are SEM. ***P<0.001 and *P<0.05, 1-way ANOVA followed by Tukey post-hoc test. n=5/group.